MECHANICS AND CONTROL
Vol. 33 No. 2 2014 http://dx.doi.org/10.7494/mech.2014.33.2.58

MARIAN SIKORA*

STUDY OF FLOW-INDUCED VIBRATION PHENOMENA IN AUTOMOTIVE SHOCK ABSORBERS

ABSTRACT

The purpose of this study was to develop a model of the dynamic behavior of a hydraulic vehicle double-tube shock absorber. The model accounts for the effects of compressibility, valve stiction, inertia, etc. and can be suitable for use in the analysis on flow-induced pressure fluctuations in the device. The author highlights all major variables to influence the output of the shock absorber, and then proceeds by performing a series of simulations using the developed model. The model is demonstrated to operate well in the large amplitude and low frequency range as well as the small amplitude and high frequency excitation operation regimes. The results are presented in the form of time histories of pressures in each fluid volume of the damper, flow rates through the valves, piston rod acceleration and force. Fast Fourier Transform (FFT) graphs are presented, too, in order to identify the major components of the pressure fluctuation phenomena in the frequency domain.

Keywords*: automotive, double-tube shock absorber, vibration, lumped parameter model*

BADANIE DRGAŃ WYWOŁANYCH PRZEPŁYWEM OLEJU W SAMOCHODOWYM TŁUMIKU HYDRAULICZNYM

Celem niniejszej pracy jest zbudowanie modelu dwururowego tłumika hydraulicznego odzwierciedlającego dynamiczne zachowanie zaworu. Stworzony model uwzględnia szereg zjawisk takich jak ściśliwość cieczy, bezwładność, siłę potrzebną do rozsunięcia dwóch równoległych płaszczyzn, pomiędzy którymi znajduje się olej (tzw. siła lepienia) i inne. Pozwala to na symulacje zjawisk dynamicznych i badanie drgań wywołanych przepływem oleju. Zostały uwzględnione wszystkie najważniejsze zmienne wpływające na generowanie drgań. Model działa poprawnie zarówno w niskich, jak i wysokich częstotliwościach. Rezultaty przeprowadzonych symulacji zostały przedstawione w postaci przebiegów czasowych ciśnienia, natężenia przepływu przez zawory oraz przyśpieszenia tłoczyska tłumika. Na wykresach częstotliwościowych widoczne są najważniejsze składowe obserwowanych drgań.

Słowa kluczowe*: przemysł samochodowy, dwururowy tłumik hydrauliczny, drgania, model o parametrach skupionych*

1. INTRODUCTION

To start with, from a design point of view conventional automotive hydraulic shock absorbers also known as vehicle dampers (Dixon 2007) as of a simple double-tube design with passive deflected disc type valves or preloaded spring valving. Although being a mature technology (the telescopic device's operating principle has not changed since the 1950s) vehicle damper often face challenging and conflicting engineering challenges. For example, it has been long recognized that the performance of suspension hydraulic shock absorbers may contribute to passenger comfort deterioration. In the view of ever increasing structural stiffness requirements imposed by vehicle OEMs (Original Equipment Manufacturers) the energy dissipation efficiency of the damper has become a research as well as an engineering challenge. As the damper separates the vehicle's body from road input through the wheel and tyre any deficiencies in the performance of the hydraulic device can contribute to the overall handling and comfort metrics of the car. It has been long recognized that any disturbances in the flow process translate into higher-frequency fluctuations in pressure transferred to the piston rod through the rigid yet compliant fluid, and then to the sprung mass (body) – noise. The pressure fluctuations are due to the damper valve's opening/closing actions while the vehicle is in motion. When integrated over the piston surface, the resulting force causes changes in fluid induced accelerations on the piston rod mass.

Efforts to model the damping force output of this device are rather well known (Lang 1977, Duym *et al.* 1997, Alonso and Comas 2006, Lee and Moon 2006, Czop *et al.* 2009, Farjoud *et al.* 2012, Ferdek and Łuczko 2012). At the same time, to the author's best knowledge, with notable hardware-based exceptions no analytical study to comprehend these flow-induced vibration phenomena has been undertaken so far (Kruse 2002, 2008). Therefore, in this study the author attempts to extend previous findings through considering the key phenomena occurring within this damper while in motion, namely, compressibility of the fluid, valve inertia and stiffness, stiction forces, and then demonstrates the capabilities of the model in a setup to copy the operating conditions of the shock absorber.

* BWI Poland Technologies sp. z o.o., Krakow, Poland; marian.sikora@bwigroup.com

2. MODELING

In this section the author highlights all key phenomena occurring inside the damper while in motion, and presents a mathematical model underlying the important variables.

2.1. Damper model

The twin-tube damper is shown in figure 1 in a setup that attempts to copy the hardware's testing conditions in a laboratory. The rod is suspended from a compliant top mount-like structure, and the external excitation x_e is applied to the reservoir tube. The output of the system is the resulting displacement of the piston rod x_{pr}. Moreover, piston rod acceleration is often a useful quantity to measure in practical analysis; it is related to the force transmitted to the car's body.

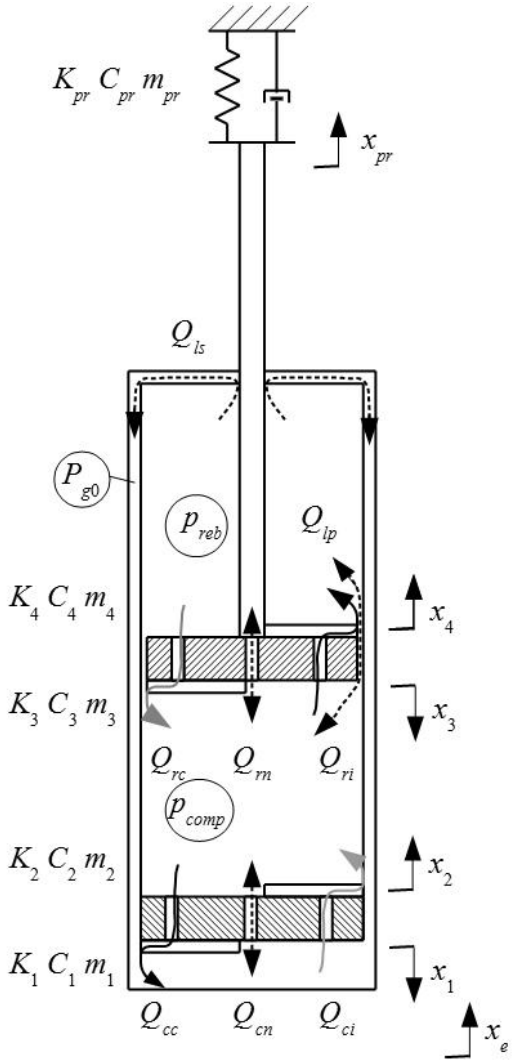

Fig. 1. Damper model, continuous black arrows – flow during rebound movement, continuous gray arrow – flow during compression movement; black dashed arrows – flow during both movements. Arrows close to x_i (i = 1,..., 4) show coordinate system orientation

By considering the forces acting on the piston, piston rod movement can be described by the following equation (1)

$$m_{pr}\ddot{x}_{pr} = C_{pr}\dot{x}_{pr} + K_{pr}x_{pr} = \\ = A_c p_{comp} - A_r p_{reb} + F_{friction} \tag{1}$$

Effectively, the motion of the piston depends on the upper top mount characteristics (K_{pr}, C_{pr}), piston rod mass m_{pr}, damper friction $F_{friction}$ and the internal pressure fluctuations. The compression pressure chamber p_{comp} operates through the surface area A_c, and the rebound pressure p_{reb} against the upper surface area of the piston A_r.

The fluid compressibility describes the equation

$$\beta = -\frac{1}{V}\frac{dV}{dp} \tag{2}$$

It can be transformed to the form

$$\beta V \frac{dp}{dt} = -\frac{dV}{dt} \tag{3}$$

where V is the oil volume in a work chamber and the right equation side is the flow rate balance.

Using (3) equation, the compression pressure can be calculated as

$$\beta_1 A_c L_c \dot{p}_{comp} = Q_{rc} + Q_{rn} - Q_{ri} - Q_{cc} + \\ + Q_{cn} + Q_{ci} + Q_{lp} + A_c\left(\dot{x}_e - \dot{x}_{pr}\right) \tag{4}$$

where $L_c = 0.5L_0$-$x_e + x_{pr}$ denotes the compression chamber length, L_0 – damper length. Moreover, the rebound pressure p_{reb} can be

$$\beta_1 A_r L_r \dot{p}_{reb} = Q_{ri} - Q_{rn} - Q_{rc} - Q_{lp} - \\ - Q_{ls} - A_r\left(\dot{x}_e - \dot{x}_{pr}\right) \tag{5}$$

where:

L_r = $0.5L_0 + x_e$-x_{pr} – the rebound chamber length,
Q_{cc} – compression-to-reservoir flow rate,
Q_{ci} – reservoir-to-compression flow rate,
Q_{cn} – base valve orifice flow rate,
Q_{ri} – compression-to-rebound flow rate,
Q_{rc} – rebound-to-compression flow rate,
Q_{rn} – flow rate through a piston valve orifice.

Finally, the leakage flow rates are Q_{lp} (piston) and Q_{ls} (rod guide). The pressures depend on the oil compressibility β_1 and the fluid volume in the chambers, respectively. As the piston is in motion, the oil is forced through the orifices and one-way valves in the piston and the base valve,

respectively. As the piston moves upward (rebound) the oil is forced through the piston into the compression chamber, and from the reservoir into the compression chamber. For comparison, as it travels downward, the oil flows into the rebound chamber and into the reservoir.

2.2. The fluid model

The fluid is assumed to be slightly compressible and Newtonian. Typical shock absorber oil properties were assumed by the author: ρ = 830 kg·m^{-3}, μ = 0.04 Pa·s, $\beta = 6.6 \cdot 10^{-10}$ Pa^{-1}. Moreover, the expansion of the cylinder wall with pressure was taken into account in the model, too. The effective compressibility is then as follows (Lang 1977)

$$\beta_1 = \beta + \frac{2r}{Es} \tag{6}$$

where r is the cylinder radius, s refers to wall thickness and E denotes the steel Young's modulus.

2.3. Disc valve model

The valve model is shown schematically in figure 2 in a manner described by Lang 1977. The model accounts for the disc stacks (valves) in the piston and the base valve, respectively.

Therefore, the effective model of the damper will utilized four of these models applied to the valves in the piston and the base valve, respectively. In general, each disc stack is characterized by mass m_i. Its stiffness and the damping are K_i, C_i, respectively. Force F_c is modeled as an additional spring of the stiffness ratio K_c activated upon the contact of the disc with the valve seat. The stiction force F_v, that is acting on the disc moving away and toward the housing is also included in the model. The motion of the disc stack mass is determined by the pressure difference across the disc Δp and through the surface area A_v. The fluid stream passing through the valve is changing the momentum. It generates additional force F_m on a given disc stack. This force depend on fluid density ρ, flow through the valve Q_i and inlet area $A_{in,i}$. Moreover, the disc is biased by the preload force F_{sp}. The force delays the opening of the valving discs, and it is an important tuning parameter of every damper design process. In the equation inertial forces should be incorporated incl. lift acceleration x_u. As such, the disc motion can be described as follows

$$m_i\left(\ddot{x}_i + \ddot{x}_u\right) + C_i\dot{x}_i + K_i x_i + \begin{Bmatrix} K_{ci}x_i, \ for \ x_i < 0 \\ 0, \ for \ x_i > 0 \end{Bmatrix} = \\ = F_{vi} + \Delta p A_{vi} + C_{fi}\,\rho\frac{Q_i^2}{A_{in\_i}} - F_{sp\_i} \tag{7}$$

where $C_f = F_{actual}/F_{predicted}$. The coefficient can be obtained experimentally. Note that not all fluid changes the momentum; there is still some longitudinal component present. The flow through the valves (Q_{cc}, Q_{cn}, Q_{ci}, Q_{rc}, Q_{rn}, Q_{ri}) is the unsteady fluid flow through the variable area passages, and it can be described by the modified Bernoulli equation

$$Q_i = C_{Di}A_i\sqrt{\frac{2\Delta p}{\rho}} \tag{8}$$

where C_{Di} denotes the dynamic discharge coefficient, A_i is the cross-section area of valve outlet, and ρ refers to the fluid density. Finally, the leakage flow (at the piston-cylinder interface and the piston-rod guide interface) is also accounted for using the laminar model

$$Q_i = \left(\frac{\Delta p b_i^3}{12\mu l_i} \pm \frac{\left(\dot{x}_e - \dot{x}_{pr}\right)b_i}{2}\right)W \tag{9}$$

where b_i is the clearance; and l_i denotes the passage length in the direction of the flow; whereas $W = \pi D_P$ is the passage width (at circumference) also, D_P refers to the diameter of the piston. This is a general equation, the sign depends on local coordinate system orientation.

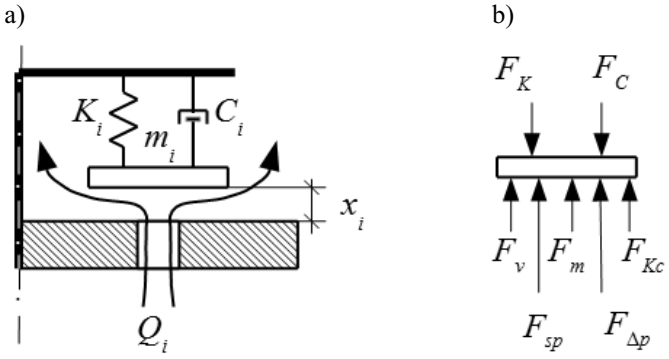

Fig. 2. Valve model: a) disc stack model, b) forces acting on valving discs

2.4. The stiction model

The model also accounts for the valve stiction phenomenon (Ezzat Khalifa and Xin Liu 1998). The oil film generates the force F_v when discs are moved away from the contacting surface, and whenever they approach the surface in which they are in contact with. By considering the pressure distribution between the disc and the contact surface, the stiction force can be obtained as

$$F_v = \frac{3\pi\mu}{2x_i^3}\frac{dx_i}{dt}R_i^4\left(1 - X_{Ai}^4 + \frac{1 - 2X_{Ai}^2 + X_{Ai}^4}{\ln X_{Ai}}\right) \tag{10}$$

where μ is fluid viscosity, R_i denotes the hydraulic radius, and the ratio $X_{Ai}^2 = A_{contact}/A_{presure\ acting}$ refers to a geometrical factor depending on the contact area and the area on which the fluid pressures act. The stiction force is proportional to the velocity and decreases rapidly with the increasing distance x_i.

2.5. System of equations

Based on equations (1) through (7) the dynamic equations governing the phenomena in the damper can be constructed as follows

$$\begin{cases} \beta_1 A_c L_c \dot{p}_{comp} = Q_{rc} + Q_{rn} - Q_{ri} - Q_{cc} + Q_{cn} + Q_{ci} + Q_{lp} + A_c\left(\dot{x}_e - \dot{x}_{pr}\right) \\ \beta_1 A_r L_r \dot{p}_{reb} = Q_{ri} - Q_{rn} - Q_{rc} - Q_{lp} - Q_{ls} - A_r\left(\dot{x}_e - \dot{x}_{pr}\right) \\ m_{pr}\ddot{x}_{pr} = -C_{pr}\dot{x}_{pr} - K_{pr}x_{pr} + A_c p_{comp} - A_r p_{reb} + F_{friction} \\ m_1\left(\ddot{x}_1 - \ddot{x}_e\right) = -C_1 v_1 - K_1 x_1 - F_{c1} + F_{v1} + \Delta p A_{v1} + C_{f1}\rho\dfrac{Q_{cc}^2}{A_{in\_1}} - F_{sp\_1} \\ m_2\left(\ddot{x}_2 + \ddot{x}_e\right) = -C_2 v_2 - K_2 x_2 - F_{c2} + F_{v2} + \Delta p A_{v2} + C_{f2}\rho\dfrac{Q_{ci}^2}{A_{in\_2}} - F_{sp\_2} \\ m_3\left(\ddot{x}_3 - \ddot{x}_{pr}\right) = -C_3 v_3 - K_3 x_3 - F_{c3} + F_{v3} + \Delta p A_{v3} + C_{f3}\rho\dfrac{Q_{rc}^2}{A_{in\_3}} - F_{sp\_3} \\ m_4\left(\ddot{x}_4 - \ddot{x}_{pr}\right) = -C_4 v_4 - K_4 x_4 - F_{c4} + F_{v4} + \Delta p A_{v4} + C_{f4}\rho\dfrac{Q_{ri}^2}{A_{in\_4}} - F_{sp\_4} \end{cases} \tag{11}$$

3. INPUT DATA

The model presented above (11) is used to analyze the flow inducted vibration phenomena. State variables are $[p_{comp}\ p_{reb}\ x_1\ x_2\ x_3\ x_4\ x_{pr}\ v_1\ v_2\ v_3\ v_4\ v_{pr}]^T$. The corresponding initial condition vector is $[6{\cdot}10^5\ 6{\cdot}10^5\ 0\ 0\ 0\ 0\ 0\ 0\ 0\ 0\ 0\ 0]$. Shortly, the simulation was conducted based on the following parameter set: $A_c = 5.0671{\cdot}10^{-4}$ m^2; $L_0 = 0.241$ m; $A_r = 4.1167{\cdot}10^{-4}$ m^2; $m_1 = 9.680{\cdot}10^{-4}$ kg; $m_2 = 1.004{\cdot}10^{-3}$ kg; $m_3 = 1.494{\cdot}10^{-3}$ kg; $m_4 = 1.919{\cdot}10^{-3}$ kg; $m_{pr} = 1.867{\cdot}10^{-1}$ kg; $C_1 = 2800$ Ns/m; $C_2 = 8$ Ns/m; $C_3 = 5600$ Ns/m; $C_4 = 900$ Ns/m; $C_{pr} = 80$ Ns/m; $K_1 = 2.8{\cdot}10^6$ N/m; $K_2 = 8{\cdot}10^3$ N/m; $K_3 = 5.6{\cdot}10^6$ N/m; $K_4 = 0.9{\cdot}10^6$ N/m; $K_{pr} = 1.3{\cdot}10^6$ N/m; $F_{friction} = 22$ N; $C_{f1} = 0.9$; $C_{f2} = 0.85$; $C_{f3} = 0.9$; $C_{f4} = 0.85$; $A_{in\_1} = 1.314{\cdot}10^{-5}$ m^2; $A_{in\_2} = 6.72{\cdot}10^{-5}$ m^2; $A_{in\_1} = 2.036{\cdot}10^{-5}$ m^2; $A_{in\_4} = 4.48{\cdot}10^{-5}$ m^2; $K_{c1} = K_{c2} = K_{c3} = K_{c4} = 10^8$ N/m; $R_1 = 0.0067$ m; $R_2 = 0.0096$ m; $R_3 = 0.0088$ m; $R_4 = 0.0109$ m; $X_{A1} = 1.0536$ m; $X_{A2} = 1.0587$ m; $X_{A3} = 1.0676$ m; $X_{A4} = 1.0428$ m; $r = 0.0127$ m; $s = 1.05$ mm; $P_{g0} = 6{\cdot}10^5$ Pa.

4. RESULTS

The numerical results are presented in the form of time histories of pressures, flow rates and the damping force output – see figure 3 and figure 4. The assumed excitation is sinusoidal: $xe = a\sin(\omega t)$. Specifically, figure 3 shows the small amplitude and higher frequency behavior (30 Hz displacement sine wave excitation) and figure 4 reveals the output of the model at large stroking amplitudes and lower frequencies (3 Hz excitation). The prescribed peak velocity of the base input was equal in either examined case – 0.378 m/s. This frequency was chosen intentionally. The lower frequency is within the range of sprung mass natural frequencies in typical passenger cars. Also, the higher frequency excitation was within the range of input frequencies identified to be the root cause of noise generation phenomenon. It should be noted the output of the modelled system (damping force) varies with the excitation frequency (see also figure 5).

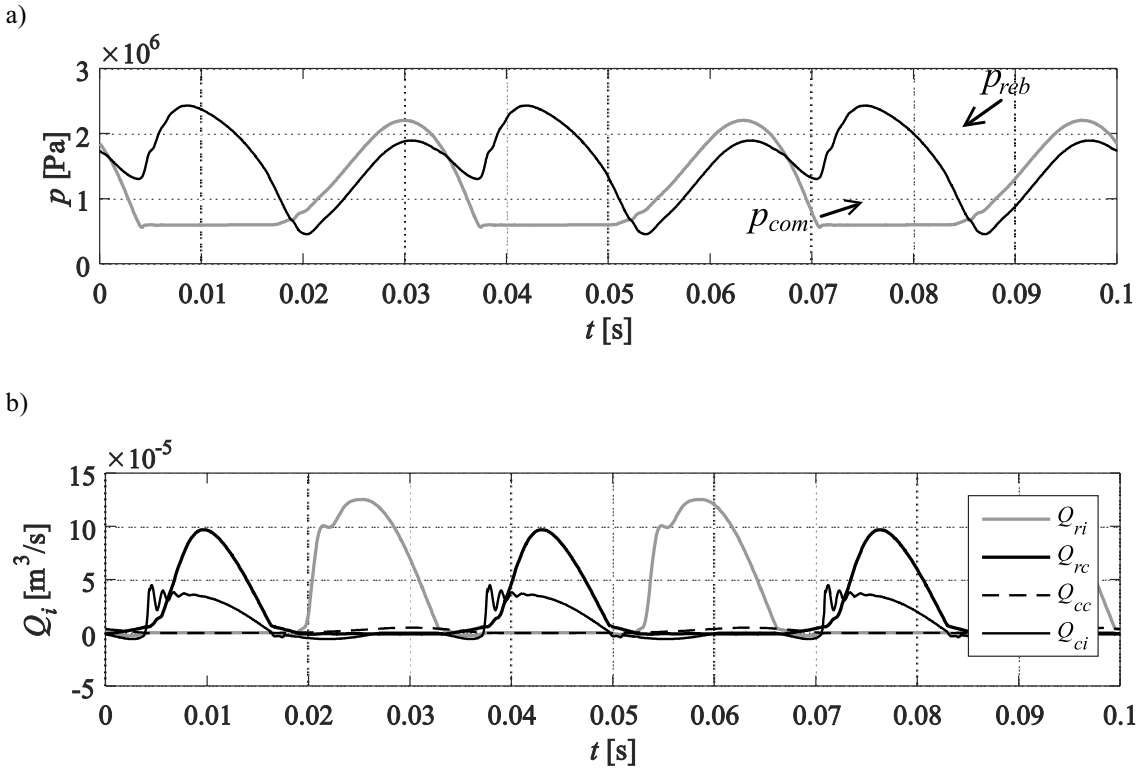

Fig. 3. Simulation result – high frequency: a) pressures, b) flow rates (valves)

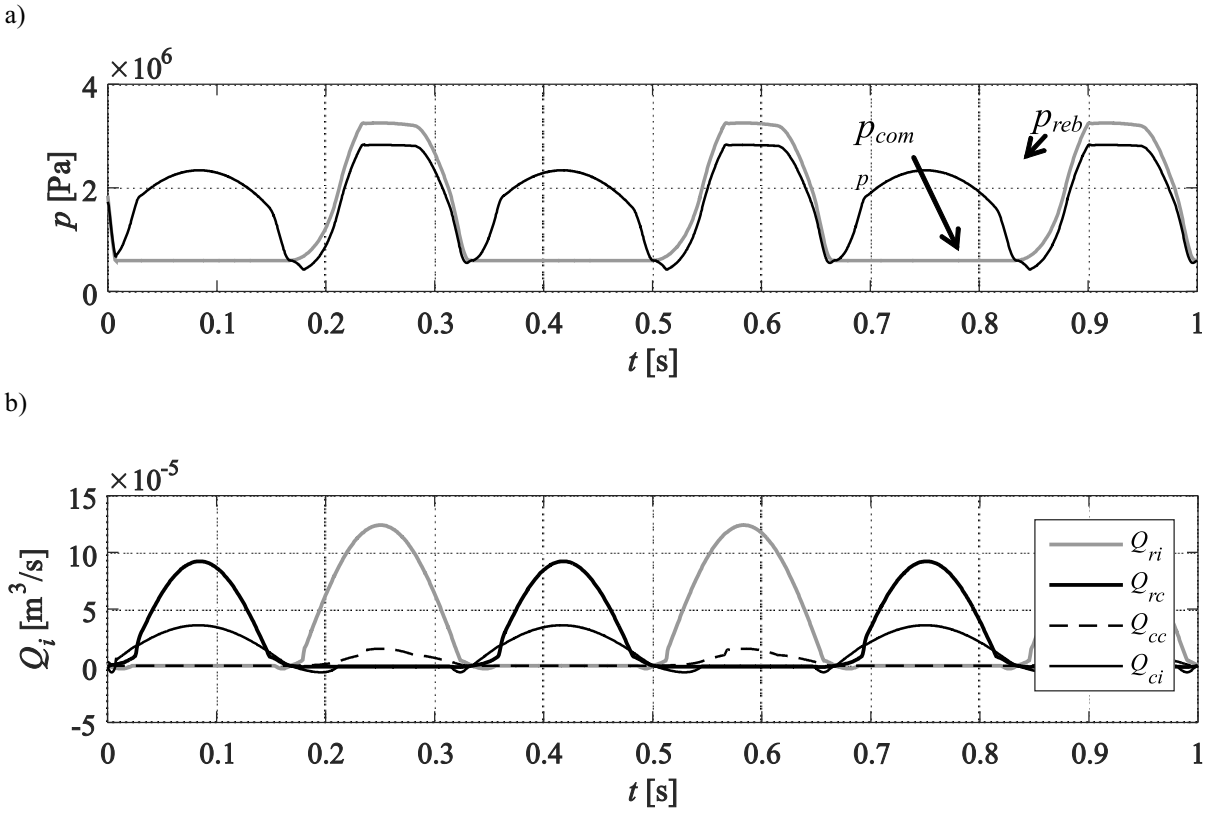

Fig. 4. Simulation result – low frequency: a) pressures, b) flow rates (valves)

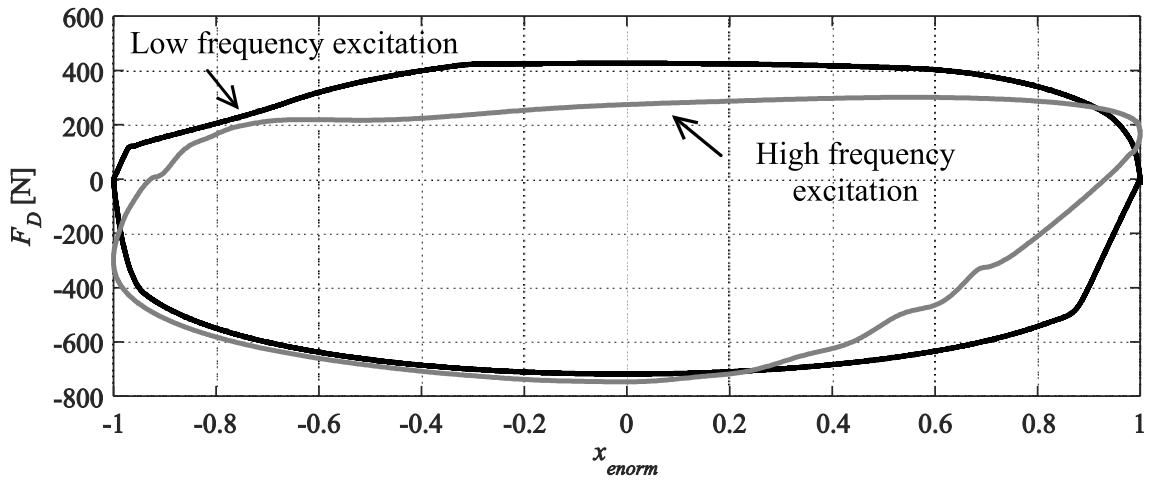

Fig. 5. Damping force vs normalized displacement loop

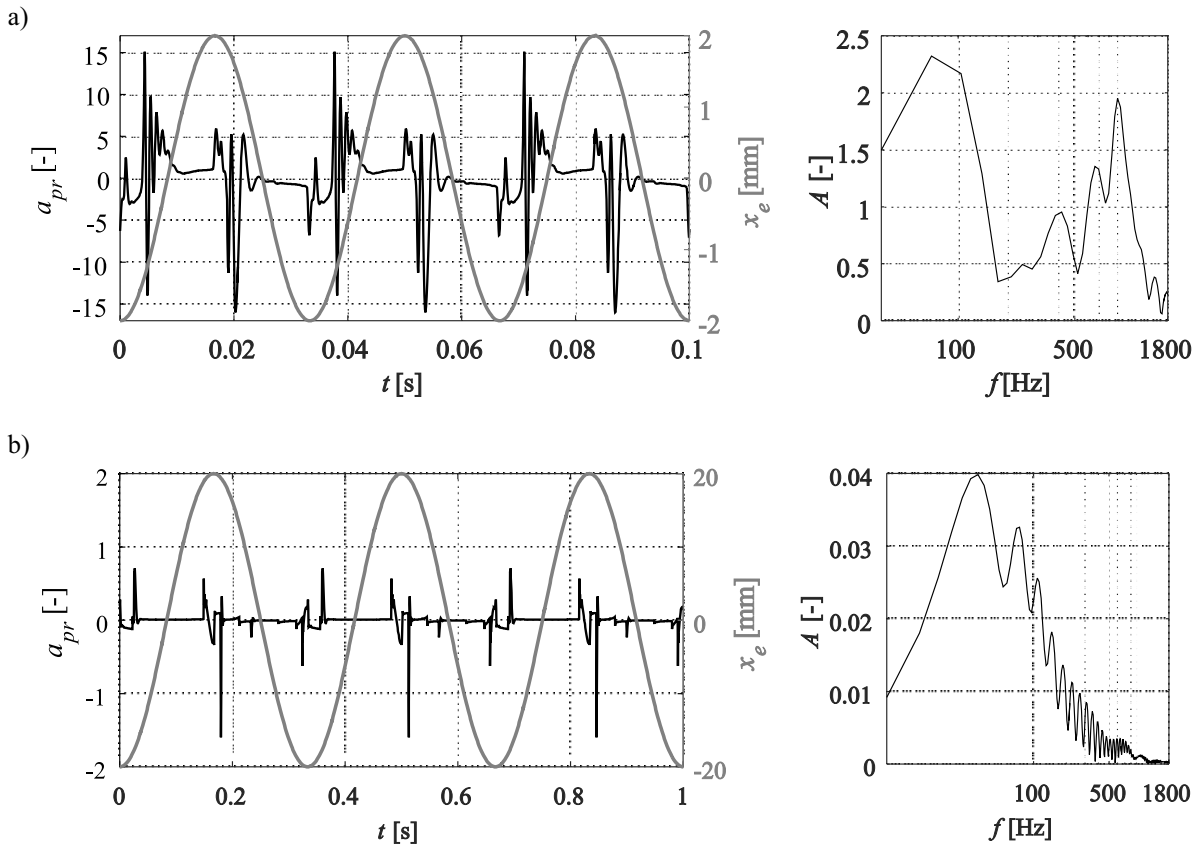

Fig. 6. Piston rod acceleration non dimensional in frequency and time domain: a) high frequency, b) low frequency

In figure 5 the excitation was normalized with respect to the amplitude to enable a direct comparison of the damping force output at different frequencies (and amplitudes) of the excitation. At the higher frequency case the dynamic behavior of the valves influences the pressure variations, and the resulting force. That is accompanied by the increased piston rod acceleration magnitude up to 15 g as seen in figure 6a. In a real vehicle the effect would be transferred to the body of the car resulting in noise. It seems the magnitude of the oscillations dominates the base valve behavior – it occurs during the transition from the compression portion of the stroking cycle to the rebound one. Some preliminary FFT (Fast Fourier Transform) analysis of the acceleration signal was calculated at the beginning of the rebound

movement, where the acceleration amplitude is maximum. The peaks below 200 Hz are connected with signal processing and excitation. The noise issue is usually connected with vibrations above this value. The dominant frequency component at appr. 890 Hz can be observed in figure 6a.

5. SUMMARY AND CONCLUSIONS

The purpose of this study was to develop a lumped parameter model of an automotive vehicle hydraulic damper. The developed model accounts for the effects of compressibility, valve stiction, inertia, etc. Mostly, it relies on geometric and material properties. It makes the model a convenient tool for fast engineering studies on the dynamic response of the mechanical valves. Preliminary results that are contained in this paper show that the model is sensitive to changes in excitation frequency. The behavior is consistent with observations and measurements on real shock absorbers in a lab.

Finally, future work will be directed towards experimental characterization of the flow-induced phenomena, the lumped parameter model validation and CFD (Computational Fluid Dynamics).

References

Alonso M., Comas Á., 2006, *Modelling a twin tube cavitating shock absorber*. Proceedings of the Institution of Mechanical Engineers, Part D: Journal of Automobile Engineering, 220(8), 1031–1040.

Czop P., Sławik D., Śliwa P., Wszołek G., 2009, *Simplified and advanced models of a valve system used in shock absorbers*. Journal of Achievements in Materials and Manufacturing Engineering, 33(2), 173–180.

Dixon J.C., 2007, *The shock absorber handbook. Second edition*. Professional Engineering Publishing Ltd and John Wiley and Sons Ltd,. 169–175.

Duym S., Stiens R., Reybrouck K., 1997, *Evaluation of shock absorber models*. Vehicle System Dynamics: International Journal of Vehicle Mechanics and Mobility 27(2), 109–127.

Ezzat Khalifa H., Xin Liu, 1998, *Analysis of stiction effect on the dynamics of compressor suction valve*. The International Compressor Engineering Conference, Paper 1221.

Farjoud A., Ahmadian M., Craft M., Burke W., 2012, *Nonlinear modeling and experimental characterization of hydraulic dampers: effects of shim stack and orifice parameters on damper performance*. Nonlinear Dynamics, 67, 1437–1456.

Ferdek U., Łuczko J., 2012, *Modeling and analysis of a twin-tube hydraulic shock absorber*. Journal of Theoretical and Applied Mechanics, 50, 2, 627–638.

Kruse A., 2002, *Characterizing and reducing structural noises of vehicle shock absorber system*. SAE Technical Paper 2002-01-1234.

Kruse A., 2008, *Analysis of dynamic pressure build-up in twin-tube vehicle shock absorbers with respect to vehicle acoustics*, SAE International, Vehicle Dynamics Expo 2008, Stuttgart.

Lang H.H., 1977, *A study of the characteristics of automotive hydraulic dampers at high stroking frequencies*, Thesis Dissertation, The University of Michigan, 19–46.

Lee C., Moon B., 2006, *Simulation and experimental validation of vehicle dynamic characteristics for displacement-sensitive shock absorber using fluid flow modelling*. Mechanical Systems and Signal Processing, 20, 2, 373–388.